THE CONTINUOUS SPECTRUM AND THE EXCITATION OF GIANT RESONANCES IN THE REACTION $^{16}O + {}^{208}Pb$

R.A. BROGLIA, G. POLLAROLO, A. VITTURI and A. WINTHER
The Niels Bohr Institute, University of Copenhagen, DK-2100 Copenhagen Ø, Denmark

and

C.H. DASSO and H. ESBENSEN
NORDITA, DK-2100 Copenhagen Ø, Denmark

Received 10 July 1979

Recent data on the inelastic scattering of ^{16}O on ^{208}Pb at 315 MeV provide a crucial test of the coherent state model of heavy ion reactions where the surface degrees of freedom are explicitly taken into account. The transfer of particles is treated as a position dependent absorption in accordance with one-particle transfer formfactors.

Recently, the reaction $^{208}Pb(^{16}O, {}^{16}O')^{208}Pb$ has been studied [1] at ≈20 MeV per nucleon. Very conspicuous structures in the continuous spectrum have been found, in particular around 10.8 MeV and in the range of 18.1–19.7 MeV. They were interpreted as arising from the excitation of isoscalar modes of different multipolaries. Data on the elastic scattering of ^{16}O on ^{208}Pb at ≈20 MeV per nucleon have also been published [2].

In the present letter we report on an analysis of these data. The model utilized was proposed in ref. [3]. It treats explicitly both the low-lying collective surface vibrations of the two interacting nuclei as well as the high-lying damped giant resonances.

The spectrum of the surface modes utilized in the calculations is for ^{208}Pb the same as used in ref. [9] except for the position of the 0^+ state. For ^{16}O it is given in the caption of fig. 1 and is similar to one used earlier. The surface–surface interaction was described in the proximity approximation [4]. The zero-point fluctuations associated with the low-lying surface modes were included by a set of random initial conditions as discussed in ref. [5].

Most of the cross section is associated with deep inelastic events with a broad energy distribution which is determined by the energy loss partly due to excitation of surface modes and partly due to the transfer of particles [6]. The energy spectrum of the ^{16}O ions detected thus receives contributions from the spectra of several heavier scattered particles, which due to particle evaporation end as ^{16}O before they reach the detector. Because of the many channels involved one expects these collisions to contribute a rather smooth background in the energy distribution. If we disregard this background we may thus treat the transfer reactions as a depopulation of the ^{16}O channel.

For the rate of transfer reactions we use the expression [7]

$$dn/dt = N(\tau/\hbar^2)[f(r)]^2 , \tag{1}$$

where τ is the collision time ($\tau \approx 0.3 \times 10^{-21}$ s) and $f(r)$ is the formfactor for single particle transfer [8].

For the latter quantity we use the approximation

$$f(r) = F/(1 + e^{\kappa(r-R)}) , \tag{2}$$

where $R = 1.25(A_a^{1/3} + A_A^{1/3})$ fm and $\kappa = 1\ \mathrm{fm}^{-1}$. The coefficient F depends on the single particle configurations in the two nuclei. A rough estimate gives $F \approx 5$ MeV. The factor N indicates the effective number of transfer channels with favourable Q-value which contribute. We have used $N = 6$.

In the numerical calculations the depopulation ac-

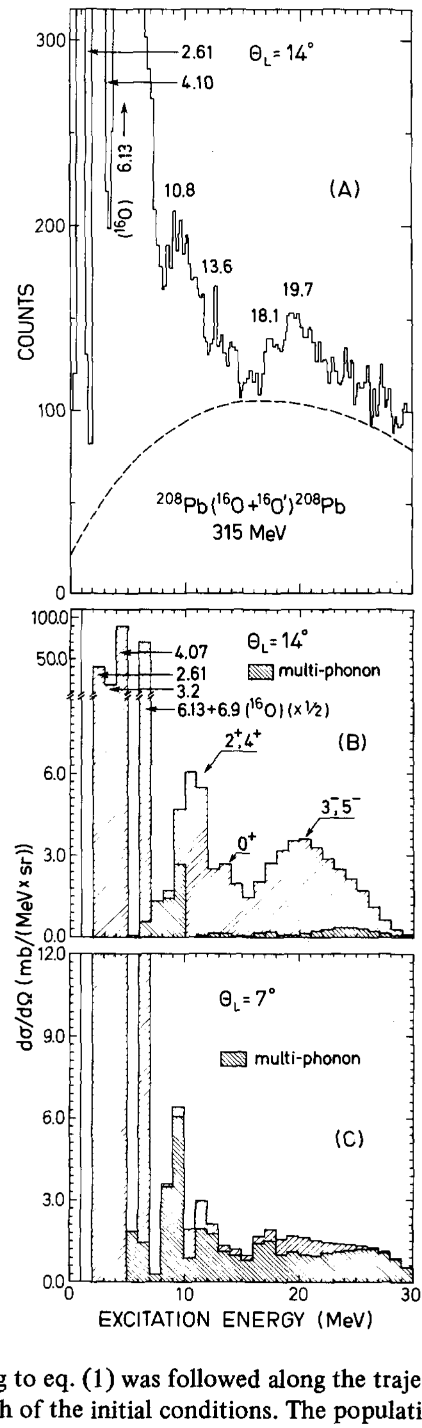

Fig. 1. Double differential inelastic cross section associated with the reaction $^{16}O + ^{208}Pb$. In (a) the experimental spectrum at the grazing angle $\theta_{lab} = 14°$ is given. In (b) and (c) the predicted "direct reaction" double differential cross sections are shown in mb/MeV sr for two different angles. The darkly shaded area corresponds to the events in which at least two harmonic oscillator quanta were absorbed. The response function of ^{16}O used was (λ, $\hbar\omega$, Γ, EWSR (%)) = (2_1^+, 69, 0, 8); (2_2^+, 23, 6, 90); (3_1^-, 61, 0, 9); (4_1^+, 23, 6, 25) where $\hbar\omega$ is the energy of the state and Γ its width, both in MeV, while EWSR (%) is the percentage of the isoscalar energy weighted sum rule associated with the excitation of the mode.

cording to eq. (1) was followed along the trajectory for each of the initial conditions. The population of the different quantum states of the surface modes was projected out of the total sample by the technique described in ref. [9].

In fig. 1b we show the resulting "direct reaction" double differential cross section $d^2\sigma/dEd\theta$ as a function of the energy loss and for the grazing angle of $\theta_{lab} = 14°$. The largest cross sections are associated with the low lying states in ^{208}Pb and in ^{16}O as indicated. All events leading to an excitation of ^{16}O of more than 10 MeV are not included in the histogram as they would lead to particle decay.

The structure seen around 11 MeV is partly due to multiple excitation of the low-lying states (hatched area) and partly to the excitation of the isoscalar giant quadrupole resonance and of the $2\hbar\omega$ component of the hexadecapole giant resonance. The shoulder at 14 MeV is due to the monopole giant resonance. The cross sections are shared in the ratio 3 : 2 : 1. While Coulomb excitation is absent for the 0^+ state and weak for the 4^+ state it accounts for 2/3 of the cross section of the 2^+ state. It is noted that this ratio has been calculated in a rather unorthodox way, and should be interpreted as an order of magnitude estimate. In fact, the ratio of 2/3 is the ratio of the inelastic cross section calculated in the range of impact parameters 11 fm $\leqslant \rho \leqslant \infty$, and the cross section calculated in the range of impact parameters $0 \leqslant \rho \leqslant 11$ fm. In both cases, both the Coulomb and nuclear interactions are included, although only Coulomb excitation is important in the range of impact parameters $\rho > 11$ fm.

The structure around 20 MeV contains little multiple excitation but mainly the excitation of the $3\hbar\omega$ component of the $\lambda = 5$ giant resonance and the octupole giant resonance. The cross section is shared in the ratio 1 : 2.

For comparison we indicate in fig. 1a the experimental data [1] which include the background from indirect reactions via transfer processes which were deleted in fig. 1b. In fig. 1c is shown the "direct" spec-

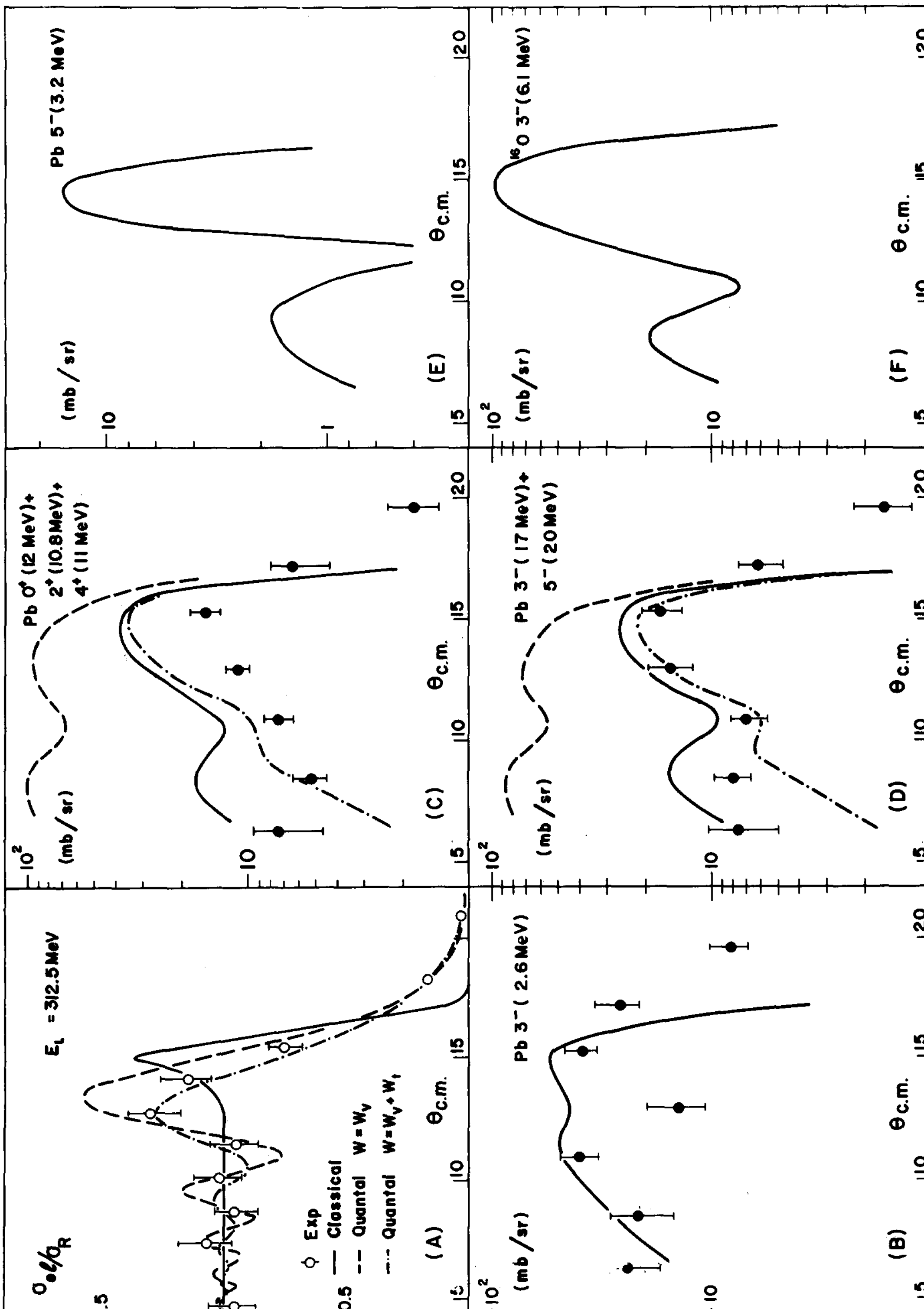

(A)
(B)
(C)
(D)
(E)
(F)
E_L = 312.5 MeV
σ_{el}/σ_R
Exp
Classical
Quantal W = W_v
Quantal W = W_v + W_t
Pb 3^- (2.6 MeV)
Pb 0^+ (12 MeV)+ 2^+ (10.8 MeV)+ 4^+ (11 MeV)
Pb 3^- (17 MeV)+ 5^- (20 MeV)
Pb 5^- (3.2 MeV)
^{16}O 3^- (6.1 MeV)
(mb/sr)
$\theta_{c.m.}$

trum at $\theta_{\mathrm{lab}} = 7°$. Besides the single excitation of the low-lying states, mainly by Coulomb excitation, the cross section is dominated by multiple excitation.

In figs. 2b–2f we show the differential cross section for the various structures seen in the spectra as full drawn curves, which are to be compared to the experimental data [1] indicated by error bars. The tendency of most of the curves to show two maxima reflects the existence of a Coulomb as well as a nuclear rainbow scattering in the average deflection function. For the giant resonances in figs. 2c and 2d we have indicated also by dash–dot curves the angular distributions associated with single phonon excitation. We have also here by dashed curves indicated the results which would apply for the single phonon excitation in the absence of the absorption (1) due to particle transfer.

In fig. 2a we display by a full drawn curve the elastic cross section utilizing the same technique as was used for the inelastic cross sections. The difference between this result and the experimental data [2], indicated by error bars, is due to the finite wave length in the relative motion. In order to carry out the quantal calculation we use for the real part of the potential the proximity potential U^N while the imaginary part should be the sum of the absorption W_{t} due to transfer and W_{v} due to excitation of surface modes. For W_{t} we should use $-\frac{1}{2}\hbar \mathrm{d}n/\mathrm{d}t$ while W_{v} is given by the analogous formula [7]

$$W_{\mathrm{v}} = -\sigma^2(\tau/\hbar^2)(\mathrm{d}U^N/\mathrm{d}r)^2 . \qquad (3)$$

The derivative of the proximity potential indicates the common radial dependence of the inelastic formfactors. The total strength σ^2 can be interpreted as the zero point fluctuation in the sum R of the nuclear radii

$$\sigma^2 = R^2 \sum_{n\lambda} \frac{(2\lambda+1)}{4\pi} \frac{\hbar\omega_\lambda(n)}{2C_\lambda(n)} , \qquad (4)$$

where the summation should be performed over all surface modes with favourable Q-value. For the present case we find $\sigma \approx 0.4$ fm. The optical model calculation is indicated by a dashed curve.

Quantal corrections to the inelastic angular distributions would give rise to a less steep decrease in the cross section beyond 15°, and would give rise to strong Coulomb nuclear interferences for the low 3^- state.

In the present investigation no attempt was made to adjust the response function of the two colliding nuclei, which was taken from ref. [9]. The good agreement with recent experiments lends confidence to the ability of the model to describe heavy ion reactions. It thus seems possible to use the model to extract more detailed information about the nuclear response function from heavy ion scattering. An analysis on the basis of distorted wave Born approximation is in general not warranted since the background may display marked structure.

Discussions with P. Doll and D. Scott are acknowledged.

References

[1] P. Doll et al., Phys. Rev. Lett. 42 (1979) 366.
[2] C. Olmer et al., Phys. Rev. C18 (1978) 205.
[3] R.A. Broglia, C.H. Dasso and A. Winther, Phys. Lett. 53B (1974) 301; 61B (1976) 113.
[4] R. Blocki, J. Randrup, W.H. Swiatecki and C.F. Tsang, Ann. Phys. 105 (1977) 427.
[5] H. Esbensen, A. Winther, R.A. Broglia and C.H. Dasso, Phys. Rev. Lett. 41 (1978) 296.
[6] R.A. Broglia, C.H. Dasso, G. Pollarolo and A. Winther, Phys. Rev. Lett. 41B (1978) 25.
[7] R.A. Broglia and A. Winther, to be published.
[8] R.A. Broglia, R. Liotta, B.S. Nilsson and A. Winther, Phys. Rep. 29B (1977) 291.
[9] R.A. Broglia et al., Phys. Lett. 87B (1979) 15.

Fig. 2. Predicted elastic and inelastic angular distributions in comparison with the experimental data. The semiclassical elastic cross section displayed in (a) was calculated as described in the text. The quantal angular distributions were calculated utilizing for the real part of the optical potential $U^N(r)$ a Saxon–Woods parametrization of the proximity potential in the tail region. The corresponding parameters are $V_0 = 54.65$ MeV, $r_0 = 1.16$ fm and $a = 0.6732$ fm. The imaginary potential $W_{\mathrm{t}} + W_{\mathrm{v}}$ contains two contributions. The first $W_{\mathrm{t}} = (60\ \mathrm{MeV}) \times \{1/[1+\exp((r-R)/(1\ \mathrm{fm}))]\}^2$ with $R = 1.25\ (A_a^{1/3} + A_A^{1/3})$ fm, is associated with the depopulation of the elastic channel because of particle transfer. The second $W_{\mathrm{v}} = 0.03, (\mathrm{MeV}^{-1}\ \mathrm{fm}^2)(\mathrm{d}U^N/\mathrm{d}r)^2$ arises from the depopulation of the elastic channel due to inelastic scattering. The optical model calculations were carried out utilizing both the absorption $W = W_{\mathrm{v}}$ and the total absorption $W = W_{\mathrm{v}} + W_{\mathrm{t}}$. In figs. (b)–(d) the angular distributions of the lowest octupole mode in Pb as well as of the structures at about 11 MeV and 20 MeV are shown (continuous line), in comparison with the data. In calculating the angular distribution shown as dashed curves in (c) and (d), no absorption due to particle transfer was included, while the dash–dot curves are the angular distributions associated with single phonon excitations.